

## Article

# Design of a Teat Cup Attachment Robot for Automatic Milking Systems

Chengjun Wang<sup>1,2</sup>, Fan Ding<sup>2,\*</sup>, Liuyi Ling<sup>1</sup> and Shaoqiang Li<sup>2</sup>

<sup>1</sup> School of Artificial Intelligence, Anhui University of Science and Technology, Huainan 232001, China; cjwang@aust.edu.cn (C.W.); lyling@aust.edu.cn (L.L.)

<sup>2</sup> School of Mechanical Engineering, Anhui University of Science and Technology, Huainan 232001, China; yolonr@163.com

\* Correspondence: 2021200572@aust.edu.cn

**Abstract:** Automatic milking systems (AMSs) for medium and large dairy farms in China require manual assistance to attach the teat cup, which greatly affects the milking efficiency and labor costs. In this regard, it is necessary to realize the automatic completion of cow teat attachment work. To address this issue, the authors developed a teat cup attachment robot for an AMS based on the theory of the solution of inventive problems (TRIZ). Specifically, we developed an enhanced algorithm for teat detection and designed a six-degree-of-freedom manipulator with integrated drive control. The design parameters were simulated and analyzed to validate their efficacy, while the rationality of the manipulator's movement during teat cup attachment was verified. The maximum displacement and angle error of the cup was 1.625 mm and 1.216 mm, respectively, as verified by the teat cup attachment error test. A dynamic response test showed that the manipulator could follow the teat of the cow in real time. The attachment time for teat cups was 21 s per cow, with a success rate of 98%. The performance of the teat cup attachment robot was capable of meeting the automatic attachment teat cup needs for medium and large dairy farms during milking.

**Keywords:** teat cup attachment robot; AMS; deep learning; TRIZ; simulation design



**Citation:** Wang, C.; Ding, F.; Ling, L.; Li, S. Design of a Teat Cup Attachment Robot for Automatic Milking Systems. *Agriculture* **2023**, *13*, 1273. <https://doi.org/10.3390/agriculture13061273>

Academic Editor: Francesco Marinello

Received: 1 May 2023

Revised: 17 June 2023

Accepted: 18 June 2023

Published: 20 June 2023



**Copyright:** © 2023 by the authors. Licensee MDPI, Basel, Switzerland. This article is an open access article distributed under the terms and conditions of the Creative Commons Attribution (CC BY) license (<https://creativecommons.org/licenses/by/4.0/>).

## 1. Introduction

From 2011 to 2021, the number of dairy cows worldwide showed an overall increasing trend. In 2021, the production of dairy products reached 3031.66 kilotons in China, an increase of 9.4% compared with 2020 [1]. The conventional milking system (CMS) is unable to satisfy human demand for milk by volume, which is inefficient and can easily cause milk and milk source pollution under improper operation. Automatic milking systems (AMSs), also called robotic milking systems, have effectively improved milk yield and quality, with a 29% increase in efficiency compared with the CMS [2,3]. Milking electricity and water consumption will also be reduced as the level of technology continues to increase [4]. Under different configurations and operating environments, an AMS has an energy consumption of 1.8–2.44 kW and a water consumption of between 25 and 36 L per 100 L of milk produced. In contrast, a 40-stall rotary milking parlor in a CMS consumes about 3.88 kilowatts of energy and consumes about 52 L of water per 100 L of milk produced [5,6]. Currently, AMSs are gradually replacing CMSs.

In the past few decades, AMS technology has developed very rapidly, where the main focus of the research is milk production, milking time, milk flow, and milk frequency [7]. Few people study the automatic cup attachment device. Based on the design of industrial robot milking, the industrial robot automatic milking system (ProFlex, Haines City, FL, USA) was released by the BouMatic corporation [8]. This system uses an industrial robotic arm to attach the teat cup. The robotic arm is located near the milking box, and one robotic arm only serves two cows. These are single-type milking machines, which is a single-milking system that is only used by one or two cows. The single-milking machine is inefficient,

has a low cost, is small in size, and is only suitable for small farms. The GEA (Germany Engineering Alliance) Group, Dusseldorf, Germany, has introduced a rotary milking robot DairyProQ [9], which has 28 to 80 milking stalls. Milking is performed with robotic arms in the milking stall, which are used for teat preparation, milking cup attachment, and spraying disinfection. Without human assistance, it can complete the milking task of 120 to 400 cows per hour, effectively reducing labor. However, each DairyProQ needs to install dozens of robotic arms, which is too expensive for medium and large dairy farms in China. The development of AMSs in China is slow. Chengdu Xindao Cheng Agriculture and Animal Husbandry Machinery Co., Ltd., Chengdu, China, produced the Xindao Cheng 9JY-2 milking machine [10], which adopts a rotary plate structure, whose pulsator frequency can be adjusted according to different cow constitutions and can choose different frequencies to improve the milking efficiency. The 9JY-2 can complete the milking task of 16–20 cows per hour. Henan Liou Animal Husbandry Equipment Technology Co., Ltd., Xinxiang, China, developed the Herringbone Liou 9J-LE O-2 × 12 milking machine [11], which adopted the automatic milking system; 24 cows can be milked simultaneously to improve the milking efficiency. However, both the 9JY-2 and 9J-LE O-2 × 12 need manual assistance attaching the teat cup.

With the increase in labor costs in China and the continuous expansion of the scale of dairy farms, there is an increasing need for dairy farms in China to replace CMSs with AMSs. The existing AMSs in China lack automatic attachment devices for dairy cows; we refer to this as a defective automatic milking system (DAMS), where the work needs to be undertaken manually, which greatly affects milking efficiency and increases the risk of musculoskeletal disorders (MSDs) for milking workers [12]. The research question is how to achieve automatic cup attachment without replacing DAMSs, liberate labor and improve milking efficiency. A. R. Frost et al. [13] designed a pneumatic robot for attaching a milking machine to a cow. The mechanical structure of this pneumatic robot adopts a parallel connecting rod structure and can realize the precise attachment of teat cups through a cylinder drive, but the working space of the pneumatic robot is too small. It cannot be matched with the existing DAMS system, and A. R. Frost et al. only conducted theoretical simulation analysis and did not produce a prototype model for verification. Scholars have not yet developed a device that can automatically attach teat cups to meet the needs of Chinese dairy farms. The purpose of this research was to design a teat cup attachment robot that can automatically attach teat cups in dairy farms equipped with a DAMS, especially for large- and medium-sized dairy farms. Since the cows are immobilized in the milking parlor and typically remain standing, sudden changes in posture due to physical illness were not considered during this study. Cows have four teats, the gaps between the teats are small, and the shape and growth angle of the teats are inconsistent. Therefore, it is extremely difficult to attach the teat cup accurately in a small space. It is also necessary to consider that the cows will move in a small range at any time in the milking parlor. Therefore, the robot needs to have the function of following the teats in real time when performing the automatic teat cup attachment. For this purpose, we designed a multi-degree-of-freedom teat cup attachment robot based on TRIZ. The rationality of its configuration design parameters met the size requirements of the milking space in medium and large dairy farms. The workspace and motion characteristics of the robot were verified using a MATLAB simulation. In order to verify the success rate of the attachment of a teat cup and whether the dynamic following of the teat could be realized when the cow moved, we designed a teat cup error experiment and a dynamic response attachment test.

## 2. System Design

### 2.1. Visual Perception

Teat detection and positioning are the keys to realizing automatic teat cup attachment. The real-time performance and accuracy of the teat cup attachment should be considered when attaching the teat cups. The detection error should be within 5 mm, and the detection time should be less than 1 s [14]. In this study, Intercompany RealSense D435 was used to

detect cow teats. RealSense D435 has small-scale and high-accuracy features that could meet the needs of this study.

Bovine teat detection and location are challenging due to the different body sizes and postures of cows, as well as the occlusion of teats by the legs of the cow and the mutual occlusion of each teat. In order to solve the above problems, a teat detection algorithm based on improved Faster R-CNN (region convolution neural network) [15] was proposed by us. Faster R-CNN is an end-to-end deep learning detection algorithm. The working principle is as follows: First, the input image is scaled and then fed into the convolutional layer to extract features, resulting in a feature map. Based on the anchor mechanism, the RPN network generates candidate bounding boxes. The feature map and candidate bounding boxes are then inputted into the ROI pooling layer to extract proposals and obtain proposal feature maps. Finally, this data is sent to the fully connected layer for target classification and coordinate regression.

As shown in Figure 1, our proposed nipple detection algorithm consists of a feature extraction backbone and a terminal for removing redundant features [16,17]. The convolutional backbone in Faster R-CNN is used as the feature extraction backbone for teat feature extraction. As the legs of the cow may obstruct its teat and different teats can also block each other, and the background, such as the udder, is also in the image, redundant features will be obtained when extracting features and will increase the computational load. The image of the teat within the bounding box obtained by the convolutional backbone is inputted to the feature suppression layer to eliminate redundant features.

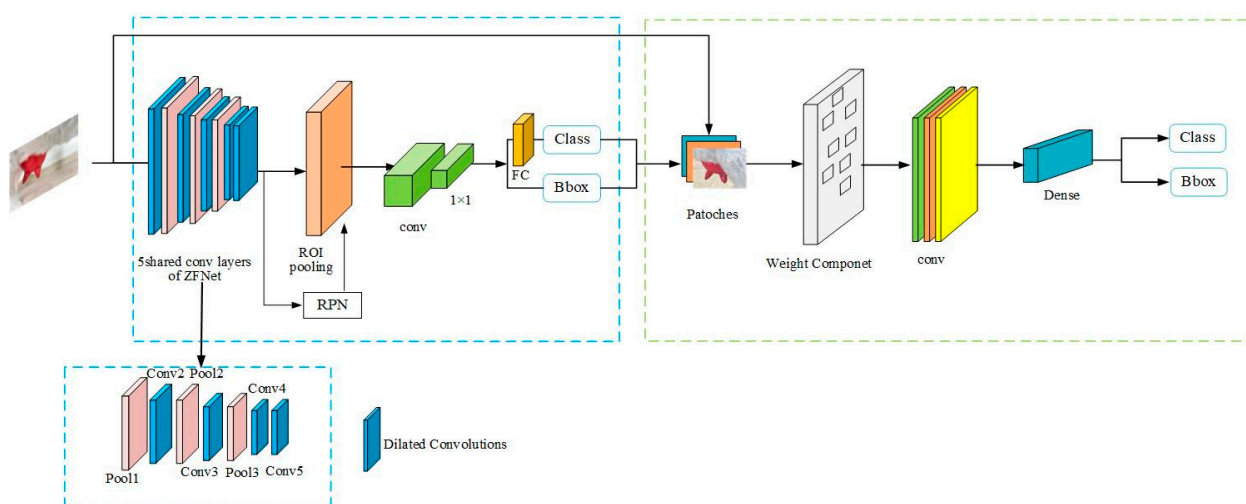


**Figure 1.** Structure of the Faster R-CNN based on the deep learning method for teat detection.

The feature suppression layer is composed of weight components and convolutional layers. Since the teat cup needs to be aligned with the end of the teat when attached, only features containing the end of the nipple are saved by the weight component, while all other redundant features are filtered out. The convolutional layer uses group-wise and point-wise convolutions to extract features separately, then fuses them and supplements feature details using  $1 \times 1$  convolutions.

To reduce the number of network parameters and improve model training speed, first, we replaced the convolution in the ZFNet (Zeiler and Fergus Net) [18] with dilated convolutions, which effectively expanded the receptive field while keeping the network parameters unchanged. Second, we replaced the feature extraction convolutional layer of Faster R-CNN with the improved ZFNet convolutional layer. Afterward, a  $1 \times 1$  convolution was chosen to replace the fully connected layer, which effectively reduces the number of network parameters and preserves the spatial structure of the image, thereby improving the accuracy.

Due to the impact of COVID-19, we could not go to a dairy farm to collect milk cow teat image data, and thus, we collected the milk cow teat model image data of different shapes in the laboratory; a total of 3000 images were collected and labeled with Lablme [19]. The dataset was divided into 2100 training sets, 600 verification sets, and 300 test sets. The implementation process and results of the algorithm for detecting cow teats based on Faster R-CNN were not within the research scope of this study, and thus, they will not be described in detail.

### 2.2. Structural Design Based on TRIZ

The theory of inventive problem solving (TRIZ, also known as TIPS) is a methodology system mainly used in structural design and optimization, which is oriented toward solving engineering problems [20–22]. Using the innovative thinking of TRIZ to analyze problems systematically and solve them through structured tools is the most effective way to realize an innovative design.

#### 2.2.1. Description of the Problem

Cause–effect chain analysis (CECE) is used to establish the logical chain between the problem’s result and its root cause, discover the cause of the problem, and identify an entry point for solving it.

Most of the existing AMSs that have the function of automatically attaching teat cups use industrial robotic arms installed on a fixed base to achieve this. However, each industrial robotic arm can only assist one or two milking parlors, making the adaptability low and the cost too high. It is not suitable for most dairy farms in China that have installed DAMSs. There is currently a lack of an automatic teat cup attachment robot that can be adapted to DAMSs in order to solve the problem of insufficient efficiency of attaching teat cups using a DAMS. The current low efficiency of DAMS teat cup attachment can be attributed to several root causes: (1) the lack of an automatic teat cup attachment robot that can be adapted to a DAMS, (2) the hand attachment for the teat cup is too inefficient, and (3) the manipulator in the AMS with the function of automatically attaching the teat cup cannot be directly adapted to the DAMS. The specific causal chain analysis is depicted in Figure 2.

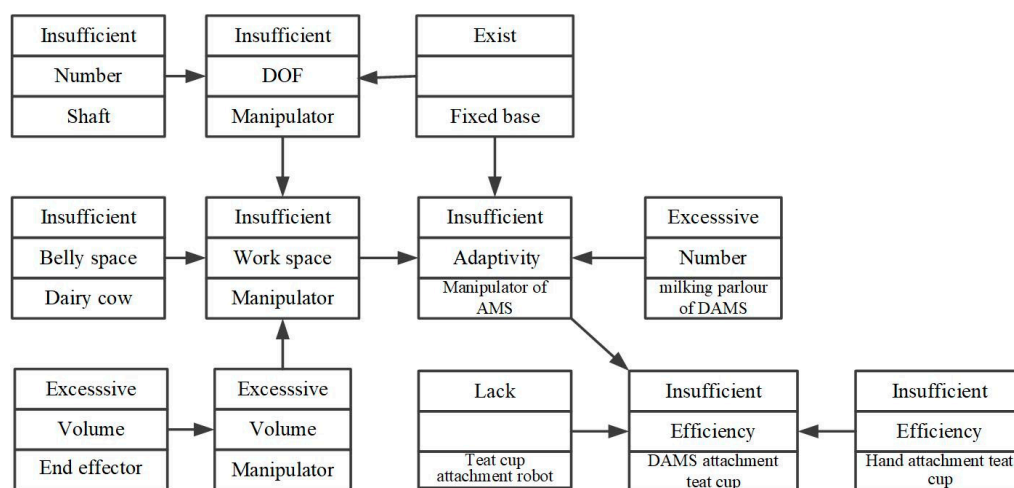


Figure 2. Cause–effect chain analysis.

Solving the problems of the manipulator in an AMS and developing a teat-cup-attaching robot was undertaken to address the issue of low efficiency in a DAMS when attaching teat cups. The problems with manipulators in an AMS are as follows: (1) the robot arm is fixed on the station and lacks overall freedom of movement; (2) an insufficient number of tandem manipulator shafts will result in a limited degree of freedom, which leads to a smaller working space; and (3) the end effector of the AMS manipulator employs

a parallel gripper to grasp both the disinfection cup and teat cup simultaneously, resulting in an excessively bulky end effector, resulting in a limited workspace.

### 2.2.2. Mechanical Arm Design Based on the TRIZ Contradiction Matrix

To solve a problem using the TRIZ method, one needs to transform an indeterminate problem into a problem model and apply different TRIZ tools for different types of problems. The contradiction matrix in the TRIZ method is designed to resolve conflicts between two different parameters. The first row and column of the contradiction matrix consist of 39 general engineering parameters, with an intersection area containing 40 invention principles to solve the corresponding contradictions [23]. The matrix is used to obtain a technical solution through the principles of invention and select the optimal solution based on actual circumstances.

We used the TRIZ contradiction matrix to solve the problem in CECE analysis. Conventionally, increasing the number of shafts (corresponding to engineering parameters are the quantity of substance) can improve the working space of the manipulator, but it will also increase its complexity (the corresponding engineering parameter is the complexity of the equipment). Reducing the volume of the end effector (the corresponding engineering parameter is the volume of the moving object) will decrease the overall volume of the manipulator, but it will also increase its complexity (the corresponding engineering parameter is the complexity of the device). We transformed the above contradictions into two pairs of technical contradictions in the TRIZ method: the deterioration parameter is no. 36, i.e., the complexity of the equipment; the improved parameters were the volume of the moving object (no. 07) and the quantity of the substance (no. 26). Based on the technical contradictions mentioned above and following the principle of solving contradiction matrix tables [24], we could derive the corresponding invention principles and establish a contradiction matrix, as shown in Table 1. We chose the appropriate principle of invention based on the actual situation and found a solution.

**Table 1.** Contradictory matrix table.

Improved Parameter	No. 36: Complexity of the Equipment
Deterioration Parameter	
No. 07: The volume of the moving object	26, 01
No. 26: The quantity of the substance	03, 13, 27, 10

We chose no. 01, i.e., the segmentation principle, to improve the system’s partition ability and achieve system transformation. The end effector comprises a teat cup gripper and a disinfection cup gripper, both of which are mounted on the rotating shaft of the rotary cylinder. The relative positions of the two can be altered via rotation. Compared with a side-by-side installation, this design can effectively reduce the size of the end effector, as shown in Figure 3. It can effectively reduce the volume of the end effector. We chose no. 03, i.e., the principle of local mass distribution, so that different parts of the object can perform distinct functions. The entire robotic arm was divided into two parts with different functions to simplify the overall robotic arm, and we replaced the missing parts with a simple attitude adjustment device. The simplified robotic arm is used to precisely adjust the position of the end effector, and the attitude adjustment device is used to expand the working space of the robotic arm. The improved mechanical arm effectively simplifies the complexity of the equipment under the premise of meeting the operational requirements. The improved mechanical arm effectively simplifies the complexity of the device while meeting the operational requirements.

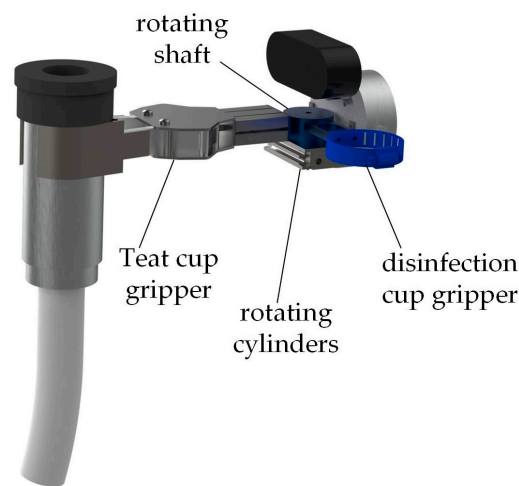
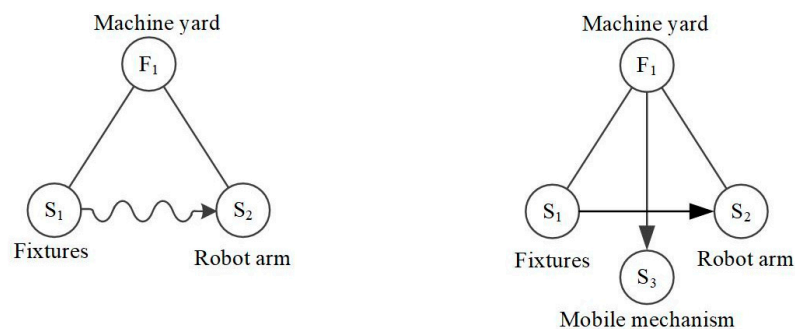


**Figure 3.** End effector.

### 2.2.3. Three-Degrees-of-Freedom Posture Adjustment System Based on a Substance-Field Analysis

Most of the AMS manipulators are fixed to the base or connected firmly to the milking parlor, and each manipulator can only be used by a maximum of two cows. Examples include the ProFlex model from BouMatic and the DairyProQ model from the GEA Group. Generally, the DAMSs of large- and medium-sized dairy farms can accommodate dozens of cows being milked simultaneously. Using one robotic arm to serve a single cow will inevitably result in high costs. For example, the smallest size of DairyProQ (capable of milking 24 cows at the same time) is priced at 20 million RMB. If one robotic arm can be used for multiple cows, the cost will be greatly decreased, although the time required for attaching the teat cup will be increased. To address this issue, we used substance-field analysis [25], as shown in Figure 4a. The fixtures restrict the movement of the robotic arm since it is mounted in the milking parlor or on the ground, which belongs to the complete substance-field model of harmful effects. We used S1.2.1 of the 76 standard solutions to introduce S3 for eliminating harmful effects, which added a three-degree-of-freedom attitude adjustment device to change the position of the robotic arm. The three-degree-of-freedom attitude adjustment device includes a ground guide rail, lifting device, and feed mechanism to increase the degree of freedom of the robot in the X-, Y-, and Z-axis directions, which enables the robotic arm to accurately adapt to DAMSs of different specifications. For example, the ground guide rail can drive the robotic arm to work on different cows, the height of the robotic arm can be adjusted using the lifting device to adapt to milking parlors of varying heights, and the feed mechanism can adjust the longitudinal position between the robotic arm and the cow to accommodate different milking parlors of varying lengths.



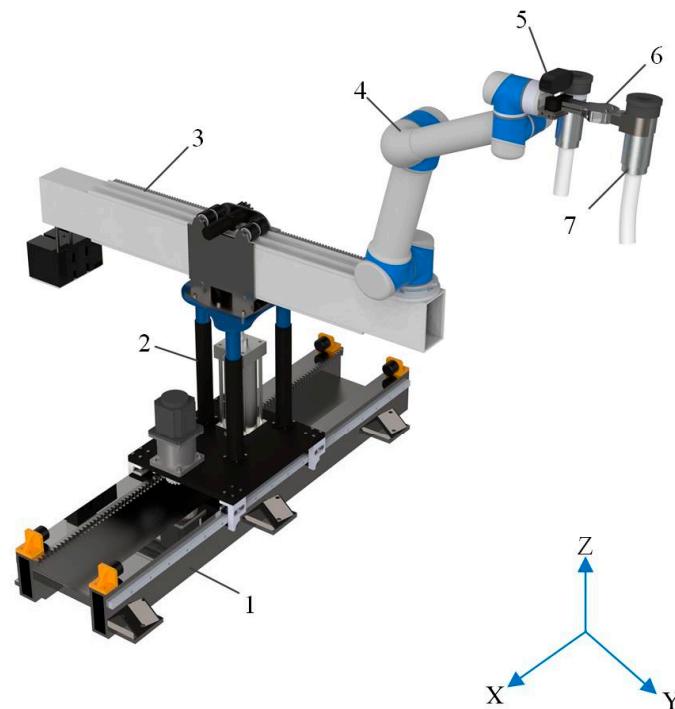
(a) . Substance-field model

(b) . The Substance-field model of general solution 2

**Figure 4.** Substance-field model analysis.

#### 2.2.4. Integration of Technical Solutions

By integrating the above schemes according to the actual working environment and working conditions of the robot, the teat cup attachment robot was innovatively designed. As shown in Figure 5, the robot mainly comprises a ground guide rail, lifting device, feed mechanism, six-degree-of-mechanical-freedom arm, and an end effector. The ground guide rail device, lifting device, and feed mechanism adjust the robotic arm along the X-, Y-, and Z-axes, and the six-degree-of-freedom robotic arm realizes the end effector to complete the setting and unloading of the cup.



1. Ground-guide rail 2. Lifting device 3. Feed mechanism
4. Six degrees of freedom robotic arm 5. RealSense D435
6. End effector 7. Milk cup

**Figure 5.** Model diagram of the teat cup attachment robot.

### 3. Simulation Analysis of Workspaces

#### 3.1. Theoretical Analysis

In order to allow the end of the manipulator to reach any teat position of the cow and make adjustments according to any posture of the cow to complete the cup-setting action, the topological mechanism was adopted for analysis. We designed a six-DOF manipulator with a topological mechanism of  $SOC\{-R\perp R\|R\|R\perp R\perp R-\}$ , which could reach any point in the working space. In order to realize multiple robots milking cows at the same time, a three-degree-of-freedom position adjustment system is connected in series under the six-degree-of-freedom manipulator arm to expand the working space of the end effector, where the specific topological mechanism of the teat cup attachment robot is  $SOC\{-P\perp P\perp P\perp R\|R\|R\perp R\perp R-\}$ .

The coordinate system between each connecting rod of the robot was established using the MD-H method [26], as shown in Figure 6, where  $\alpha_{i-1}$  refers to the torsion angle between  $n$  connecting rods, specifically referring to the angle between the  $Z_i$ -axis and the  $Z_{i-1}$ -axis;  $a_{i-1}$  is the length of the connecting rod, specifically the distance from the  $Z_i$ -axis to the  $Z_{i+1}$ -axis along  $x_i$ ;  $d_i$  refers to the linkage bias angle, specifically the distance from the  $x_{i-1}$ -axis to the  $x_i$ -axis along the  $Z_i$ -axis; and the knuckle angle  $\theta_i$  specifically refers

to the angle from the  $x_{i-1}$ -axis to the  $x_i$ -axis around the  $Z_i$ -axis. The maximum working radius of the six-DOF manipulator is 882 mm. The specific MD-H parameters of the teat cup attachment robot are shown in Table 2.

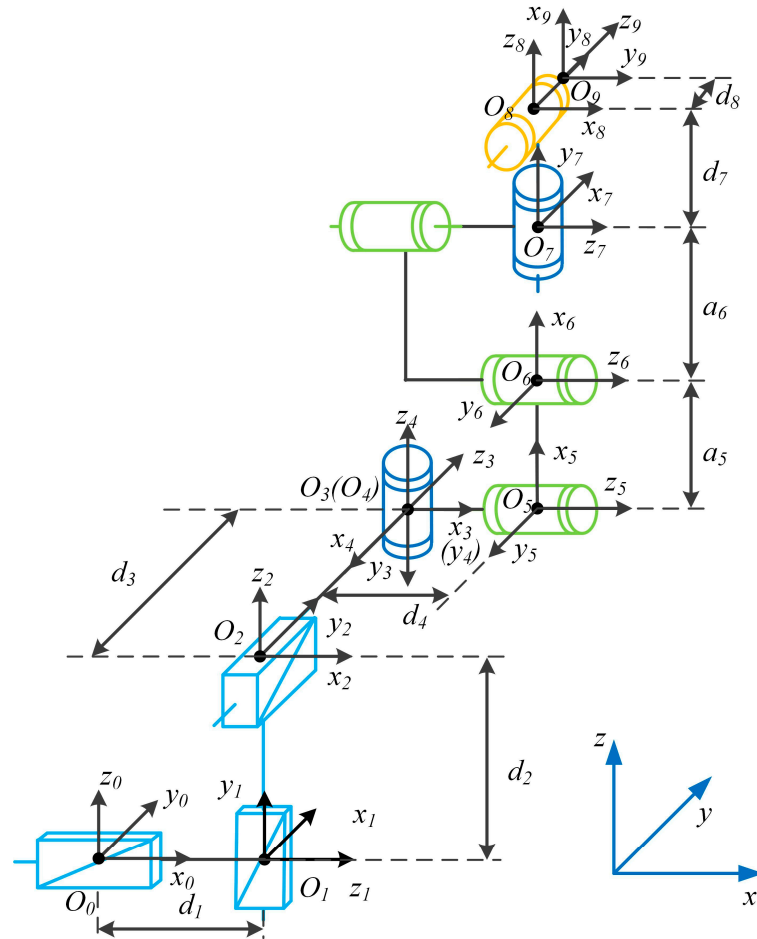


Figure 6. D-H coordinates of the teat cup attachment robot.

Table 2. MD-H parameters of the robot.

$i$	$\alpha_{i-1}$	$a_{i-1}/mm$	$d_i/mm$	$\theta_i$	Range of Variables
1	$-90^\circ$	0	$d_1$	0	0~1500 mm
2	$90^\circ$	0	$d_2$	$90^\circ$	300~1500 mm
3	$90^\circ$	0	$d_3$	0	0~1000 mm
4	$90^\circ$	0	$d_4$ (135)	$\theta_4$	$-175\sim175^\circ$
5	$-90^\circ$	$a_5$ (421)	0	$\theta_5$	$-175\sim175^\circ$
6	0	$a_6$ (394)	0	$\theta_6$	$-175\sim175^\circ$
7	0	0	$d_7$ (92)	$\theta_7$	$-175\sim175^\circ$
8	$-90^\circ$	0	$d_8$ (70)	$\theta_8$	$-175\sim175^\circ$
9	$-90^\circ$	0	0	$\theta_9$	$-360\sim360^\circ$

The pose equation of the manipulator’s end effector establishes the transformation matrix between the coordinate system  $i$  and its adjacent links relative to  $I - 1$  through a generalized transformation. The formula is as follows:

$${}^{i-1}_i T = Rot(x, \alpha_{i-1}) Trans(a_{i-1}, 0, 0) Rot(z, \theta_{i-1}) Trans(0, 0, d_1) \tag{1}$$

A  $4 \times 4$  matrix was utilized to express the general formula for connecting the rod transformation in Formula (1):

$${}^i T_{i-1} = \begin{bmatrix} c_i & -s_i & 0 & a_{i-1} \\ s_i \cos \alpha_{i-1} & c_i \cos \alpha_{i-1} & -\sin \alpha_{i-1} & -d_i \sin \alpha_{i-1} \\ s_i \sin \alpha_{i-1} & c_i \sin \alpha_{i-1} & \cos \alpha_{i-1} & -d_i \cos \alpha_{i-1} \\ 0 & 0 & 0 & 1 \end{bmatrix} \tag{2}$$

In Formula (2),  $c_i = \cos \theta_i$  and  $s_i = \sin \theta_i$ .

We then introduced the D-H parameters as presented in Table 2 according to the D-H coordinate system and the principle of the homogeneous transformation matrix; the position matrix of each joint was obtained as follows:

$$\begin{aligned} {}^0 T_1 &= \begin{bmatrix} 1 & 0 & 0 & 0 \\ 0 & 1 & -1 & -d_1 \\ 0 & 1 & 0 & 0 \\ 0 & 0 & 0 & 1 \end{bmatrix}, {}^1 T_2 = \begin{bmatrix} 0 & -1 & 0 & 0 \\ 0 & 0 & 1 & d_2 \\ -1 & 0 & 0 & 0 \\ 0 & 0 & 0 & 1 \end{bmatrix}, {}^2 T_3 = \begin{bmatrix} 1 & 0 & 0 & 0 \\ 0 & 0 & 1 & d_3 \\ 0 & -1 & 0 & 0 \\ 0 & 0 & 0 & 1 \end{bmatrix}, \\ {}^3 T_4 &= \begin{bmatrix} c_4 & -s_4 & 0 & 0 \\ 0 & 0 & -1 & d_4 \\ s_4 & c_4 & 0 & 0 \\ 0 & 0 & 0 & 1 \end{bmatrix}, {}^4 T_5 = \begin{bmatrix} c_5 & -s_5 & 0 & a_5 \\ 0 & 0 & 1 & 0 \\ -s_5 & -c_5 & 0 & 0 \\ 0 & 0 & 0 & 1 \end{bmatrix}, {}^5 T_6 = \begin{bmatrix} c_6 & -s_6 & 0 & a_6 \\ s_6 & c_6 & 0 & 0 \\ 0 & 0 & 1 & 0 \\ 0 & 0 & 0 & 1 \end{bmatrix}, \\ {}^6 T_7 &= \begin{bmatrix} c_7 & -s_7 & 0 & 0 \\ s_7 & c_7 & 0 & 0 \\ 0 & 0 & 1 & d_7 \\ 0 & 0 & 0 & 1 \end{bmatrix}, {}^7 T_8 = \begin{bmatrix} c_8 & -s_8 & 0 & 0 \\ 0 & 0 & 1 & 0 \\ -s_8 & -c_8 & 0 & 0 \\ 0 & 0 & 0 & 1 \end{bmatrix}, {}^8 T_9 = \begin{bmatrix} c_9 & -s_9 & 0 & 0 \\ 0 & 0 & 1 & 0 \\ -s_9 & -c_9 & 0 & 0 \\ 0 & 0 & 0 & 1 \end{bmatrix}, \tag{3} \end{aligned}$$

By setting  $c_{56} = \cos(\theta_5 + \theta_6)$ ,  $s_{56} = \sin(\theta_5 + \theta_6)$ ,  $c_{567} = \cos(\theta_5 + \theta_6 + \theta_7)$  and  $s_{567} = \sin(\theta_5 + \theta_6 + \theta_7)$ , according to the principle of matrix multiplication, the pose matrix of the end of the robot compared with the initial fixed platform was obtained. Using a forward kinematics solution, we obtained the matrix of coordinates of the parameters of the final position, namely, Formula (4). The terminal position and pose points of the robot relative to the base coordinate system are as follows (Formula (4)).

$$\begin{aligned} {}^0 T_9 &= {}^0 T_1 {}^1 T_2 {}^2 T_3 {}^3 T_4 {}^4 T_5 {}^5 T_6 {}^6 T_7 {}^7 T_8 {}^8 T_9 = \\ &\begin{bmatrix} s_4(c_9(s_8 - c_8c_{567}) - s_9s_{567}) & -s_9((c_4s_8 - s_4c_8c_{567}) - s_4c_9s_{567}) \\ s_{567}(c_9(c_4 - c_8)) + c_{567}(s_9 + c_9c_8c_4) - s_4s_5 & s_{56}(s_9(c_8 + c_4) - s_7) + c_{56}(s_9(s_7 - c_4c_8) - c_4) - s_4s_8s_9 \\ s_9s_{567} - c_8c_9s_{567} & c_9c_{567} + c_8s_9s_{567} \\ 0 & 0 \\ c_4c_8 + s_5s_8c_{567} & -d_3 - d_7c_4 - s_4(a_5 + a_6c_5) \\ c_8s_4 + s_{56}(s_8c_7 + c_4s_7) + c_{56}(s_7 - s_8c_7c_4) & d_2 - d_1 - d_4 - a_6(s_5 - c_4c_5) + a_5c_4 - d_7s_4 \\ s_8s_{567} & d_2 - d_4 - a_6s_5 \\ 0 & 1 \end{bmatrix} \tag{4} \\ \begin{bmatrix} 0_x \\ 0_y \\ 0_z \\ 1 \end{bmatrix} &= {}^0 T_9 \begin{bmatrix} 0 \\ 0 \\ 0 \\ 1 \end{bmatrix} = \begin{bmatrix} -d_3 - d_7c_4 - s_4(a_5 + a_6c_5) \\ d_2 - d_1 - d_4 - a_6(s_5 - c_4c_5) + a_5c_4 - d_7s_4 \\ d_2 - d_4 - a_6s_5 \\ 1 \end{bmatrix} \end{aligned}$$

### 3.2. Simulation Verification

#### 3.2.1. Workspace Verification

According to the parameters and kinematic parameters of the teat cup attachment robot, the Monte Carlo method [27] was adopted to solve the workspace, and MATLAB simulation verification was carried out. A total of 100,000 random values in each revolute joint angle range were substituted into Formula (4). The three-dimensional cloud image of the working space of the robot was obtained, as shown in Figure 7a, and the two-dimensional point cloud image of the X–Y, X–Z, and Z–Y planes is shown in Figure 7b–d.

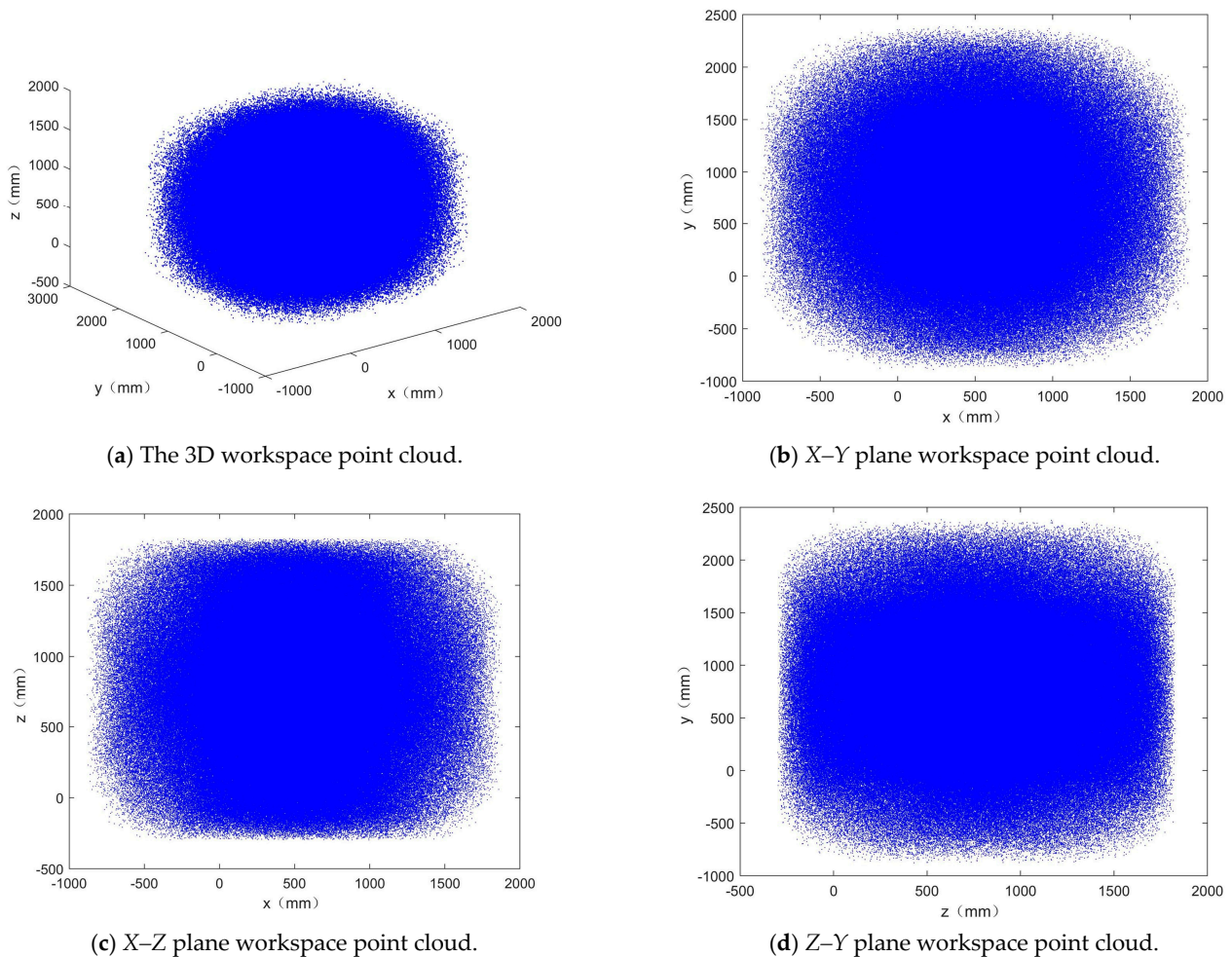


**Figure 7.** Working space point clouds of the robot. (a) shows the point cloud diagram in three-dimensional space, and (b–d) are the sections of the point cloud diagram in the X–Y, X–Z, and Z–Y planes, respectively.

Figure 7 shows that the teat cup attachment robot had a working space range of (−819 mm, 1819 mm) on the X-axis, (−819 mm, 2318 mm) on the Y-axis, and (−229 mm, 1819 mm) on the Z-axis. The breed of dairy cows in most Chinese dairy farms is Holstein-Friesian, with a rear udder width ranging from 168.2 to 222.6 mm and a distance between the udder and ground of 440 to 610 mm [28]. The heights of DAMS milking parlors in medium and large dairy farms generally range from 440 to 1000 mm, while the width of each milking parlor is 1.2 m [29]. The simulation analysis indicated that the robot met China's common requirements for cup spacing in a DAMS.

### 3.2.2. Motion Trajectory Simulation

In order to verify the stability and continuity of the teat cup attachment robot during its motion, quintic polynomial interpolation [30] was used for the interpolation calculation to design the trajectory of the end of the robot arm, and the simulation was verified using MATLAB. Because the milking robot proposed in this study is a nine-degree-of-freedom redundant robot, in which the three-degree-of-freedom attitude adjustment device is mainly used for an initial attitude adjustment, in order to meet the actual requirements, only the motion trajectory of the six-degree-of-freedom manipulator was analyzed and the results are presented in this section.

Kai Li et al. [31] showed that when pollinating kiwifruit, it took 5 s for the robotic arm to reach the target macaque peach blossom with the maximum joint angular velocity of 0.105 rad/s. Based on the above studies, the maximum angular joint velocity of the milking robot arm was designed to be  $\omega_{max} = 0.105$  rad/s. The maximum range of motion of the joint was  $-175\sim 175^\circ$ .

Let the joint angles at some point be  $\theta(t)$ , and the start and end joint angles be  $\theta_s$  and  $\theta_e$ . The equation based on a quintic polynomial was as follows:

$$\theta(t) = a_0 + a_1t + a_2t^2 + a_3t^3 + a_4t^4 + a_5t^5 \tag{5}$$

$$\begin{cases} \theta(t_s) = \theta_s \\ \theta(t_e) = \theta_e \\ \dot{\theta}(t_s) = 0 \\ \dot{\theta}(t_e) = 0 \\ \ddot{\theta}(t_s) = 0 \\ \ddot{\theta}(t_e) = 0 \end{cases} \tag{6}$$

$$\begin{cases} \theta(t_s) = a_0 \\ \theta_e = a_0 + a_1t_e + a_2t_e^2 + a_3t_e^3 + a_4t_e^4 + a_5t_e^5 \\ \dot{\theta}(t_s) = a_1 \\ \dot{\theta}(t_e) = a_1 + 2a_2t_e + 3a_3t_e^2 + 4a_4t_e^3 + 5a_5t_e^4 \\ \ddot{\theta}(t_s) = 2a_2 \\ \ddot{\theta}(t_e) = 2a_2 + 6a_3t_e + 12a_4t_e^2 \end{cases} \tag{7}$$

Equations (6) and (7) were substituted into Equation (5) to obtain the trajectory planning equation based on quintic polynomial interpolation:

$$\begin{cases} a_0 = \theta_s \\ a_1 = \dot{\theta}(t_s) = 0 \\ a_2 = \frac{1}{2} \ddot{\theta}(t_s) = 0 \\ a_3 = \frac{20\theta_e - 20\theta_s - (8\dot{\theta}_e + 12\dot{\theta}_s)t_e + (\ddot{\theta}_e - 3\ddot{\theta}_s)t_e^2}{2t_e^3} = \frac{10\theta_e}{t_e^3} \\ a_4 = \frac{30\theta_s - 30\theta_e + (14\dot{\theta}_e + 16\dot{\theta}_s)t_e - (\ddot{\theta}_e - 3\ddot{\theta}_s)t_e^2}{2t_e^4} = -\frac{15\theta_e}{t_e^4} \\ a_5 = \frac{12\theta_e - 12\theta_s - (6\dot{\theta}_e + 6\dot{\theta}_s)t_e + (\ddot{\theta}_e - \ddot{\theta}_s)t_e^2}{2t_e^5} = \frac{6\theta_e}{t_e^5} \end{cases} \tag{8}$$

According to the above solution, the quintic polynomial interpolation equation was obtained, and the trajectory planning of the joint space was carried out using MATLAB 2020a. Figure 8a–e shows the position curve of the end, position curve of the joint, orientation curve of the joint, speed curve of the joint, and acceleration curve of the joint, respectively.

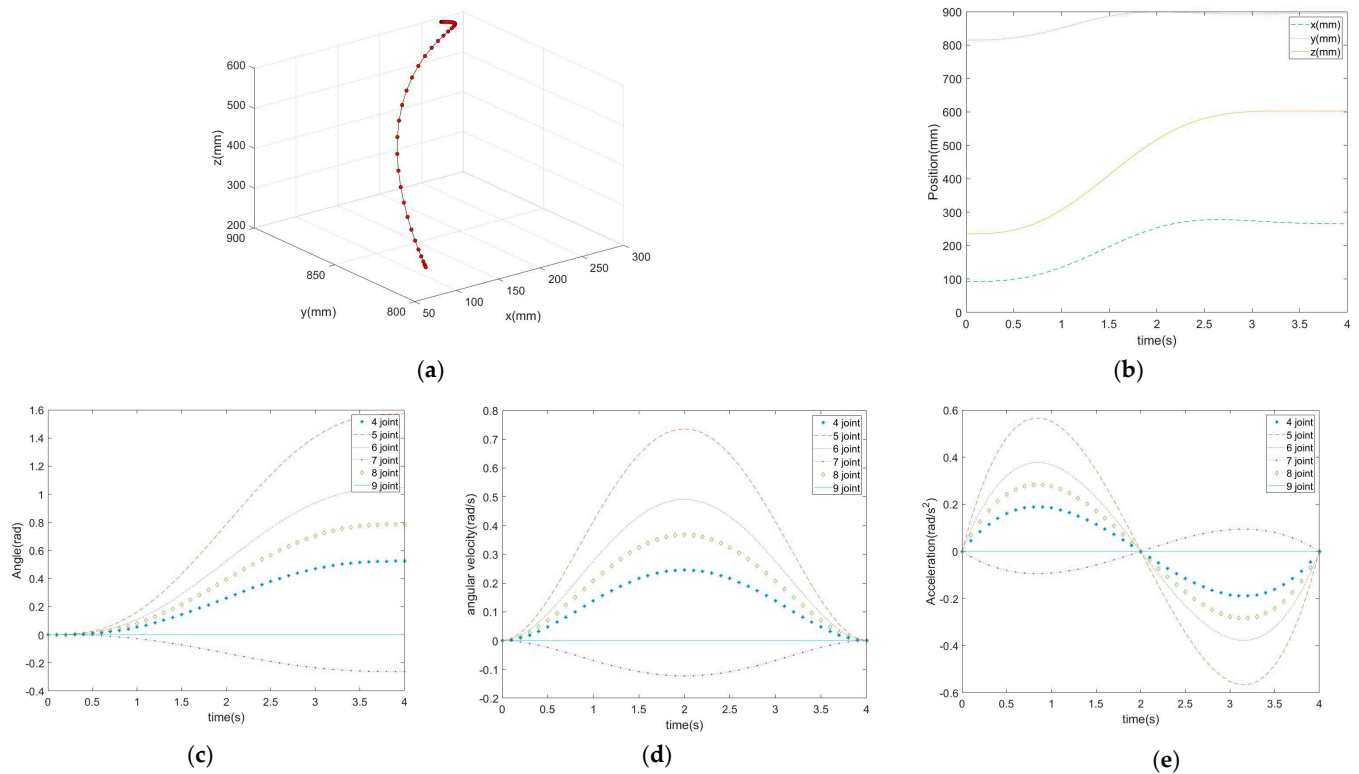


**Figure 8.** Simulation results of trajectory planning. (a) Cartesian space trajectory planning. (b) Position curve of the end. (c) Orientation curve of the joint. (d) Velocity curve of the joint. (e) Acceleration curve of the joint.

As can be seen from Figure 8, the displacement, velocity, and acceleration of each joint of the teat cup attachment robot were smooth and continuous in the process of movement, and the end displacement was smooth without abrupt shaking; even if the joint angular acceleration is  $\omega > \omega_{max}$ , the acceleration curve will not change abruptly, which demonstrates that the design of the six-degrees-of-freedom manipulator has a reasonable structural design and excellent motion characteristics.

## 4. Experimental Verification

### 4.1. Establishment of the Experimentation Platform

Due to objective environmental limitations, the experiment was carried out in the Artificial Intelligence Laboratory of Anhui University of Science and Technology, Huainan, China. Simplified measures were adopted in the experiment, and cows were replaced by models with a fixed height, where the model size was 450 mm × 350 mm × 750 mm, as shown in Figure 9. Due to the different shapes and sizes of cow teats, different types of silicone teats were used instead, as shown in Figure 10. Different types of silicone nipples have different colors and different heights that range from 5 to 7 cm. Because there is an angle between the cow's teat and the udder, we stuck adhesive tapes of different heights on the sides of the silicone teats so that there was an inclination when they adhered to the cow frame model, as shown in Figure 11. Since the posture of the cow frame model was fixed and the model was always in the fan orientation of 180° in front of the robot, there was no need to install the three-degree-of-freedom attitude adjustment device. Instead, the ground guide rail was used to replace the three-degree-of-freedom attitude adjustment

device, and a simplified version of the teat cup attachment robot prototype was built, as shown in Figure 12.

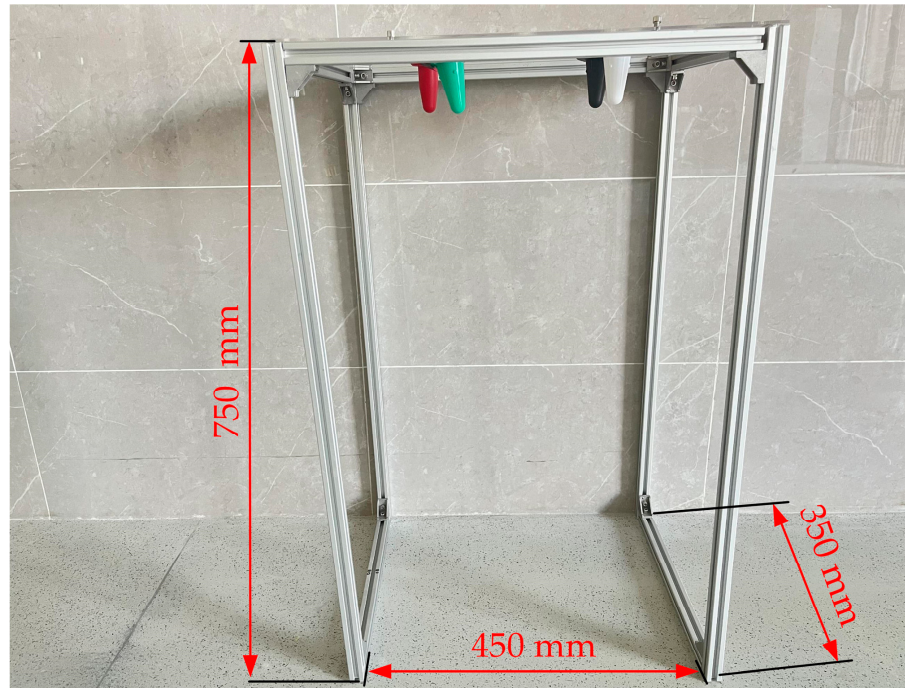


Figure 9. Cow frame model.



Figure 10. Silicone teat.

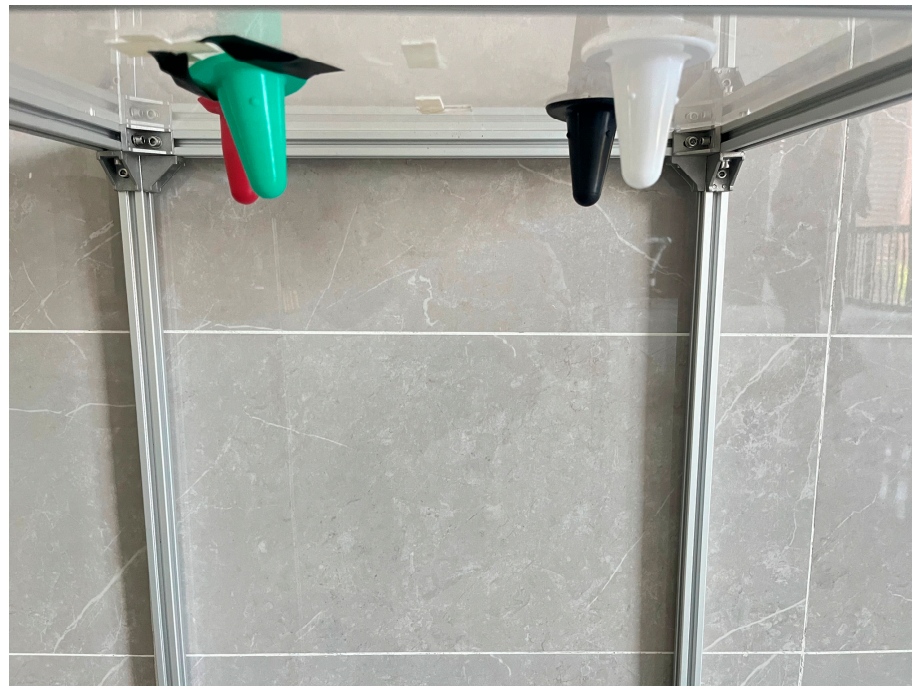


Figure 11. Pacifier location map.

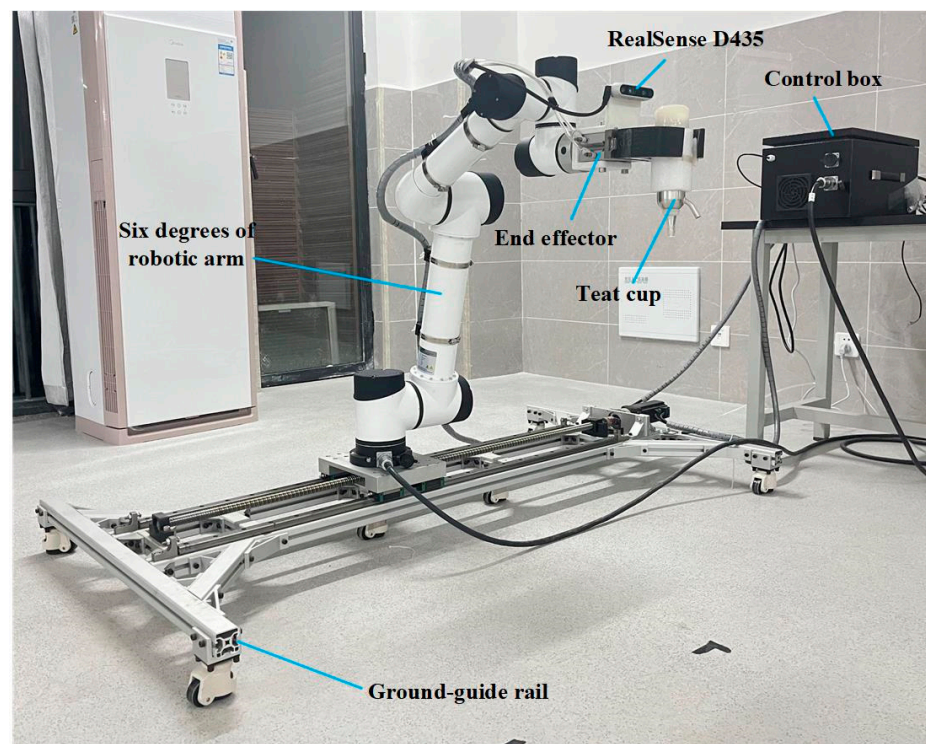


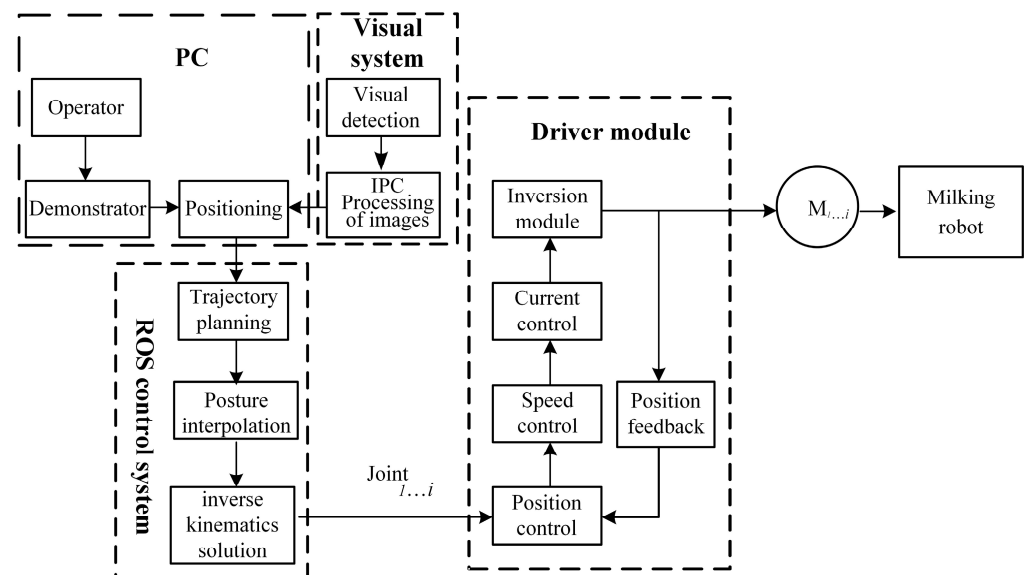
Figure 12. Simplified teat cup attachment robot prototype.

The control system of the teat cup attachment robot included a controller (IRC-M, Hefei Hagong Tu Nan Zhi Control Robot Co., Ltd., Hefei, China; IRC-M parameters as shown in Table 3), main control chip model TMS320F28335, and six motor drivers (RDM-15D80-AE, Shenzhen Taikete Intelligent Servo Technology Co., Ltd., Shenzhen, China) that were based on FPGA technology combined with an ARM and DSP structure.

**Table 3.** The control motherboard parameters.

Parameter	CPU	RAM	CPU Clock Speed	Hard Disk Drive	Real-Time System	Operating System	Jitter Delay
Data	i7-4500 U	8 GB	2.6 GHz	128 GB SSD	Support	Ubuntu16.04 LTS + Xenomai	30 $\mu$ s

The control system mainly comprised a PC, vision system, ROS manipulator control system, and drive module. The PC mainly assisted with the basic parameters and switch control of the robot. The vision system realized the identification and positioning of the cow teat. It sent the position information of the target teat to the ROS system, which carried out trajectory planning and calculated the interpolation points of the robot arm in real time. Then, the interpolation information was transmitted to the master controller. The drive module of the master controller first read the current position information of each motor and sent corresponding control signals to the encoder of each motor according to the current position to control the joint movement and change the position of the end of the manipulator, as shown in Figure 13.

**Figure 13.** Control system diagram of the teat cup attachment robot.

#### 4.2. Experimental Results

A simplified prototype teat cup attachment robot was used to cup the model teat on the frame of the cow model to verify the performance of the teat cup attachment robot in the Artificial Intelligence Laboratory of Anhui University of Science and Technology, Huainan, Anhui Province, China.

In the robot milking operation process, visual recognition, teat cup fetching, and teat cup attachment are the key steps that affect work efficiency. Our main research purpose was to design a teat cup attachment robot that can help DAMSs to realize the function of automatically attaching a teat cup. The success rate of teat cup attachment is one of the key criteria for verifying the performance of a teat cup attachment robot. The success rate of teat cup cupping is verified by the error test of teat cup attachment and the dynamic response attaching test. The teat cup attachment efficiency of the teat cup attachment robot was tested by mimicking the actual attaching process.

After several attaching teat tests, we found that the average attachment time for a single teat was 3–4 s, and the time to complete the attachment for a cow was about 21 s.

#### 4.2.1. Teat Cup Attachment Error Test

During the milking process, the robotic arm needs to put the teat cup on the cow's teat several times. Verifying whether the robot can accurately attach the teat cup is an important indicator for evaluating the teat cup attachment robot's performance. In this study, the variable control method was adopted to test the set value and the actual value of the sleeve cup of the robotic arm. To begin, we manually calibrated the optimal attachment point for each teat on the robot and recorded it as a reference point. The calibration values that yielded the best results for all four teats are shown in Table 4.

**Table 4.** The calibration values.

End Pose Coordinates	x/mm	y/mm	z/mm	R <sub>x</sub> /°	R <sub>y</sub> /°	R <sub>z</sub> /°
Teat 1	−429.072	146.419	419.700	39.381	−86.562	131.546
Teat 2	−421.632	156.815	419.301	54.385	73.251	143.704
Teat 3	−429.225	147.105	420.427	63.508	−69.724	120.463
Teat 4	−430.354	155.250	420.708	35.564	−93.552	152.107

We carried out multiple sets of cup attachment tests on four silicone teats with different specifications and angle attachments on the cow frame model. Then, we compared the test values with the set values and recorded the maximum error value and its position point for each teat cover attached, as shown in Table 5. The test process diagram is shown in Figure 14, and the actual coordinate diagram of the robot software interface is shown in Figure 15.

**Table 5.** Robot coordinate position values.

End Pose Coordinates	x/mm	y/mm	z/mm	R <sub>x</sub> /°	R <sub>y</sub> /°	R <sub>z</sub> /°	Max Error (mm/°)
Teat 1	−429.537	146.921	420.655	39.542	−85.935	131.904	0.955/0.627
Teat 2	−422.792	156.987	420.352	55.236	−72.914	142.807	1.160/0.897
Teat 3	−430.850	146.234	421.059	63.932	−70.318	119.832	1.625/0.631
Teat 4	−431.106	156.021	419.589	36.781	−94.534	151.863	1.119/1.216

As can be seen from Table 5, the maximum displacement error of the teat cup was 1.625; the angle error was 1.216; the average diameter of the teat of the cow was 24.4 mm; the diameter of the head of the teat cup was about 26 mm [32]; and the teat cup was made of silicone or rubber products with good toughness, which fully met the requirements of the actual milking operation. In the teat cup attachment error test, a total of 140 experiments were conducted on a cow model, including 100 static attachment tests and 40 dynamic attachment tests where the experimenter moved the cow model within a small range in real time while the robot attached the teat cup. Out of these tests, there were three failures, resulting in an overall teat cup attachment success rate of 98%. The reason for the failures was that the teat cups slipped from the silicone nipple after attachment. After analysis, it was found that the failure factor had nothing to do with robot positioning accuracy but was related to an insufficient depth of attachment and issues with the silicone teat manufacturing process.

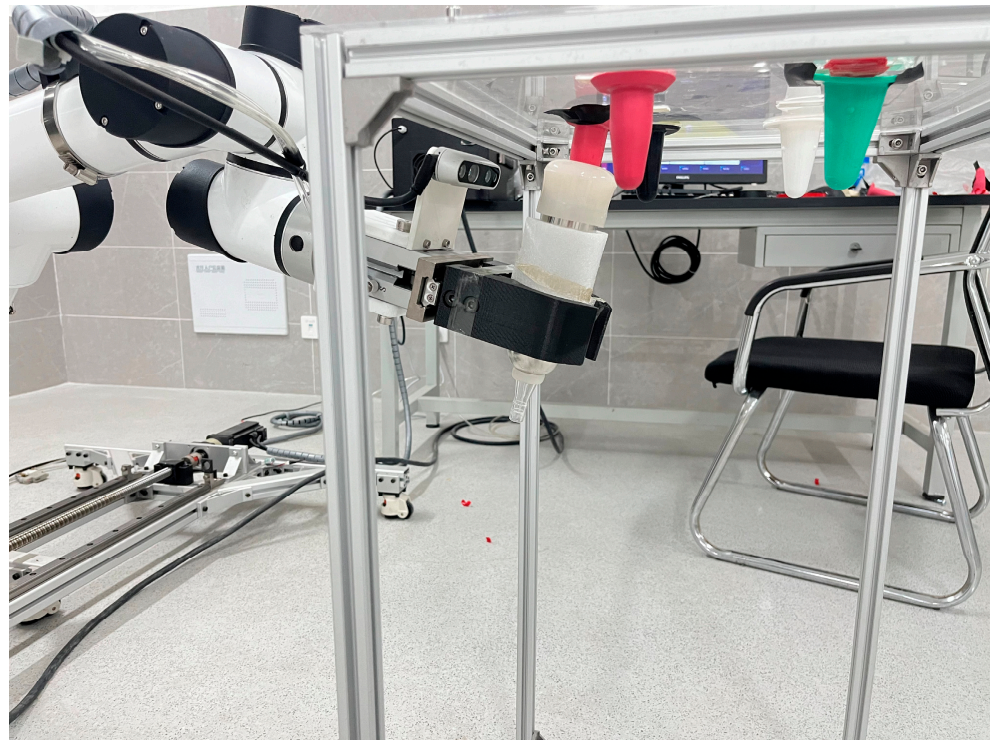


Figure 14. Teat cup error test photo.



Figure 15. Actual coordinate diagram in the software interface. The term "位置" refers to displacement, while "姿态" denotes angle.

#### 4.2.2. Dynamic Response Test

During the process of attaching teat cups, the robot must be able to respond in real time to any sudden movements made by the cow that may cause a shift in the target point. It is imperative that we verify whether the robot arm can effectively track these movements and successfully complete its task.

To test the robot's real-time tracking capability, we conducted a dynamic response experiment using an attached teat cup as our target. First, we established various trajectory points for the cow's movement along its path (as shown in Figure 16a). The manual handling of the cow began at its initial point and followed this trajectory to simulate its movements within a milking parlor. Once the robot arm positioned itself under the target

teat with readiness to attach, we initiated actions on our cow frame model and observed whether the robot followed the teat in real time. We also recorded the center position of the teat cup when the cow frame model was at its set point.

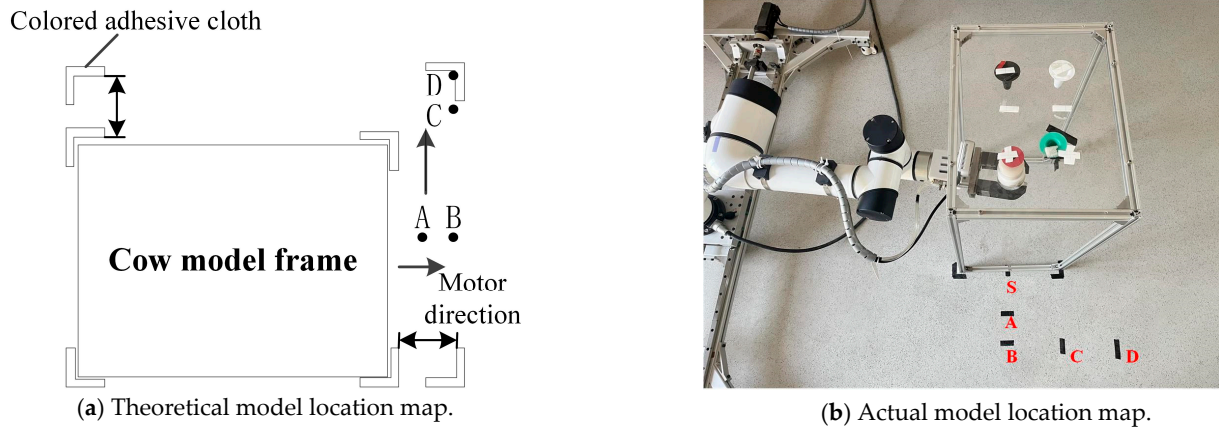


**Figure 16.** Location map of the cow model: (a) the movement direction of the model and the initial position of each preset point relative to the model; (b) the actual position of each point. A–S is the location point of the cow model, S is the start point, and D is the end point. The cow model moves from S to A to B to C and finally to D.

For the initial position of the cow model, the red teat was designated as the target teat. X and Y were defined as preset parameters for the center of the teat, while X1 and Y1 were defined as the real-time cup-center position parameters, as presented in Table 6.

**Table 6.** Center position of the teat cup.

Coordinate Value	X/mm	Y/mm	X1/mm	Y1/mm
Starting point	0	0	0	0
A point	50	0	50.725	0.725
B point	100	0	100.189	1.811
C point	100	50	102.016	53.675
D point	100	100	101.507	99.206

It can be seen from Figure 17 that the robot arm could follow the model in real time, and its error was 3.675 mm at most, as shown in Table 6. Due to the corresponding errors caused by the human movement of the model, it was impossible for the model to truly reach the predetermined point. Excluding the influence of human error, the robot arm could accurately realize the cupping of the moving target.



**Figure 17.** Dynamic response of the robot cup test diagram: (a–e) the movement of the model from the origin to point D and the following real-time process of the robot arm.

## 5. Discussion

Compared with the double box milking robot developed by BouMatic [33], which can only attach teat cups to two cows, our robot is capable of changing its position through a ground guide rail to milk multiple cows. Compared with the pneumatic robot for attaching a milking machine developed by A. R. Frost et al. [13], which has a small working space, our robot utilizes a six-degree-of-freedom serial robotic arm and offers a larger working space that better meets the needs of various farms.

In order to verify the feasibility of the teat cup attachment robotic automated setting cup program, we designed a cup test. According to the teat cup error test results, the positioning error of the sleeve cup of the mechanical arm could cover the gap between

the teat cup and the teat. It can be seen that the success rate of cupping reached 98% after conducting 140 cupping experiments, but this was only under laboratory conditions. In the actual environment, the different teat shapes of cows, occlusion between teats, and lighting in the dairy farm will also affect the recognition and positioning of the target teat by the visual system. During milking, cows are usually confined in a separate barn, which can limit their movements and facilitate milking. However, in order to make cows comfortable, cows generally have some space in the barn, and thus, there is a possibility that the target teat will move when the robot arm attaches the cup. The robot design should have the automatic follow function to ensure the correct attachment of the teat cup. The dynamic response cup test, which was designed in this study, verified that the teat cup attachment robot could follow the target and solve the problem of inaccurate cup setting when cows are moving.

The experiment showed that the time for a single teat attachment was 3–4 s, and the time for attaching all four teats of a cow was about 21 s. It took about five times longer to attach a teat cup to a cow than to attach a single teat. Usually, a cow only has four teats. However, when a teat cup is being attached to a cow, the attachment of the first teat cup will affect subsequent attachments. This can result in smaller spacing between teats, which may interfere with both the mechanical arm movement and visual detection of the teats.

Our performance verification of the robot was limited to laboratory tests, and the actual dairy farm environment is significantly more complex than that of a controlled setting. For instance, cows have varying nipple shapes and appearances, each cow has unique physical characteristics, and their posture in the milking parlor may not conform to theoretical standards, which can impact the efficiency of the robot. A dairy farm is poorly illuminated, and the teat detection system may not accurately identify each teat due to mutual occlusions. However, we took these issues into consideration during the design of the detection algorithm.

## 6. Conclusions

This paper introduces a teat cup attachment robot, whose mechanical structure was innovatively designed based on TRIZ theory, and the detection device was established based on the teat detection system of dairy cows. In this study, a simplified prototype was built, which integrated a visual sensing system, a six-degree-of-freedom manipulator, and a mechatronic control system to perform teat cup attachment. Experiments in the laboratory showed that the success rate of the robot arm could reach 98%, and the average time of four teats (cows have four teats) was 21 s. Compared with the 16-bail robotic rotary developed by DeLaval [34], which takes nearly 70 s to attach the teat cup sleeve to the cow completely, our designed teat cup attachment robot greatly improved the attachment efficiency. The proposed teat cup attachment robot could meet the requirements of the efficiency and success rate of teat cup attachment. This innovative technology effectively reduces labor requirements and minimizes the risk of musculoskeletal disorders for milking workers.

Our future work will involve gathering authentic cow teat data for training, enhancing the detection algorithm, and optimizing its real-time detection speed and accuracy. The ground guide rail of the current simplified prototype will be replaced with a three-degree-of-freedom attitude-adjusting device, and a nine-degree-of-freedom teat cup attachment robot proposed in the theoretical design will be built to cope with the real dairy farm environment. We aim to develop prototypes that cater to actual dairy farm requirements and conduct experiments in real-world dairy farms.

**Author Contributions:** C.W. designed a three-dimensional model of the robot and wrote the original draft; F.D. designed the simulation and experiments and visual perception system; L.L. designed the control system; S.L. performed the experiments and data analysis and interpretation. All authors have read and agreed to the published version of the manuscript.

**Funding:** This research was funded by the Special Work of National Innovation Methods of China, grant number (2018IM010500); the Research and the Development Fund of the Institute of Environ-

mental Friendly Materials and Occupational Health, Anhui University of Science and Technology, grant number (ALW2022YF06); and the Anhui Province University Collaborative Innovation Project of China, grant number (GXXT2019018).

**Institutional Review Board Statement:** Not applicable.

**Data Availability Statement:** Not applicable.

**Conflicts of Interest:** The authors declared no potential conflicts of interest with respect to the research, authorship, and/or publication of this article.

## References

1. Yang, Z.; Zhu, W.; Cheng, G. Dairy Market Review 2021 and Forecast 2022 trends. *Chin. J. Anim. Sci.* **2022**, *58*, 273–276. [CrossRef]
2. de Koning, C.J.A.M. Milking Machines. Robotic Milking. In *Encyclopedia of Dairy Sciences*, 2nd ed.; Fuquay, J.W., Ed.; Academy Press: New York, NY, USA, 2011; pp. 952–958.
3. Bijl, R.; Kooistra, S.; Hogeveen, H. The Profitability of Automatic Milking on Dutch Dairy Farms. *J. Dairy Sci.* **2007**, *90*, 239–248. [CrossRef] [PubMed]
4. Gaworski, M. Implementation of Technical and Technological Progress in Dairy Production. *Processes* **2021**, *9*, 2103. [CrossRef]
5. Rasmussen, J.B. Electricity and water consumption by milking. *ICAR Tech. Ser.* **2005**, *10*, 147–151.
6. Calcante, A.; Tangorra, F.M.; Oberti, R. Analysis of electric energy consumption of automatic milking systems in different configurations and operative conditions. *J. Dairy Sci.* **2016**, *99*, 4043–4047. [CrossRef]
7. Cogato, A.; Bršćić, M.; Guo, H.; Marinello, F.; Pezzuolo, A. Challenges and Tendencies of Automatic Milking Systems (AMS): A 20-Years Systematic Review of Literature and Patents. *Animals* **2021**, *11*, 356. [CrossRef]
8. Jiang, H.; Wang, W.; Li, C. Innovation, practical benefits and prospects for the future development of automatic milking systems. *Front. Agric. Sci. Eng.* **2017**, *4*, 37–47. [CrossRef]
9. GEA DairyProQ. Available online: <https://dairylane.ca/products/robotic-systems/gea-dairyproq/> (accessed on 28 December 2022).
10. Zheng, G.; Shi, Z.; Teng, G. Research Progress on Facility and Equipment Technology for Dairy Farming in China. *Chin. J. Anim. Sci.* **2019**, *55*, 169–174. [CrossRef]
11. Qin, H. Milking machine collection. *Farm Mach.* **2021**, *11*, 41–43. [CrossRef]
12. Douphrate, D.I.; de Porras, D.G.R.; Nonnenmann, M.W.; Hagevoort, R.; Reynolds, S.J.; Rodriguez, A.; Fethke, N.B. Effects of milking unit design on upper extremity muscle activity during attachment among U.S. large-herd parlor workers. *Appl. Ergon.* **2017**, *58*, 482–490. [CrossRef]
13. Frost, A.R.; Street, M.J.; Hall, R.C. The development of a pneumatic robot for attaching a milking machine to a cow. *Mechatronics* **1993**, *3*, 409–418. [CrossRef]
14. Ben Azouz, A.; Esmonde, H.; Corcoran, B.; O’Callaghan, E. Development of a teat sensing system for robotic milking by combining thermal imaging and stereovision technique. *Comput. Electron. Agric.* **2015**, *110*, 162–170. [CrossRef]
15. Ren, S.; He, K.; Girshick, R.; Sun, J. Faster R-CNN: Towards real-time object detection with region proposal networks. *IEEE Trans. Pattern Anal. Mach. Intell.* **2017**, *39*, 1137–1149. [CrossRef]
16. Zheng, C.; Zhu, X.; Yang, X.; Wang, L.; Tu, S.; Xue, Y. Automatic recognition of lactating sow postures from depth images by deep learning detector. *Comput. Electron. Agric.* **2018**, *147*, 51–63. [CrossRef]
17. Chu, P.; Li, Z.; Lammers, K.; Lu, R.; Liu, X. Deep learning-based apple detection using a suppression mask R-CNN. *Pattern Recognit. Lett.* **2021**, *147*, 206–211. [CrossRef]
18. Zeiler, M.D.; Fergus, R. Visualizing and Understanding Convolutional Networks. In Proceedings of the Computer Vision—ECCV 2014, Cham, Switzerland, 6–12 September 2014; pp. 818–833.
19. Russell, B.C.; Torralba, A.; Murphy, K.P.; Freeman, W.T. LabelMe: A Database and Web-Based Tool for Image Annotation. *Int. J. Comput. Vis.* **2007**, *77*, 157–173. [CrossRef]
20. Abramov, O.; Kogan, S.; Mitnik-Gankin, L.; Sigalovsky, I.; Smirnov, A. TRIZ-based approach for accelerating innovation in chemical engineering. *Chem. Eng. Res. Des.* **2015**, *103*, 25–31. [CrossRef]
21. Spreafico, C.; Russo, D. TRIZ Industrial Case Studies: A Critical Survey. *Procedia CIRP* **2016**, *39*, 51–56. [CrossRef]
22. Sheu, D.-L.D.; Chiu, M.-C.; Cayard, D. The 7 pillars of TRIZ philosophies. *Comput. Ind. Eng.* **2020**, *146*, 106572. [CrossRef]
23. Lin, S.Y.; Wu, C.T. Application of TRIZ inventive principles to innovate recycling machine. *Adv. Mech. Eng.* **2016**, *8*, 1687814016647303. [CrossRef]
24. Jou, Y.-T.; Lin, W.-T.; Lee, W.-C.; Yeh, T.-M. Integrating the TRIZ and Taguchi’s Method in the Optimization of Processes Parameters for SMT. *Adv. Mater. Sci. Eng.* **2013**, *2013*, 830891. [CrossRef]
25. Bultey, A.; Beuvron, F.D.B.D.; Rousset, F. A substance-field ontology to support the TRIZ thinking approach. *Int. J. Comput. Appl. Technol.* **2007**, *30*, 113–124. [CrossRef]
26. Deng, H.; Zhu, L.; Wang, J.; Chen, M.; Wu, H.; He, C. Kinematics modeling and trajectory planning of KUKA manipulator based on MATLAB. *J. Phys. Conf. Ser.* **2022**, *2216*, 012056. [CrossRef]
27. Dam, T.; Chalvatzaki, G.; Peters, J.; Pajarinen, J. Monte-Carlo Robot Path Planning. *IEEE Robot. Autom. Lett.* **2022**, *7*, 11213–11220. [CrossRef]

28. Zhao, K.; Kang, Z.; Fan, H.; Rao, H.; Sun, W.; Wang, J.; Lai, S. Correlation Research between Anogenital Distance and Milk Production in Chinese Holstein Dairy Cattle. *J. Sichuan Agric. Univ.* **2022**, *40*, 645–648. [[CrossRef](#)]
29. Gao, J.; Li, C.; Pang, J.; Peng, Y.; Sun, L.; Yu, F. Development and application of 9JZP-80 high efficiency rotary milking machine. *Heilongjiang Anim. Sci. Vet.* **2022**, *648*, 50–55. [[CrossRef](#)]
30. Zhao, J.; Han, T.; Ma, X.; Ma, W.; Liu, C.; Li, J.; Liu, Y. Research on Kinematics Analysis and Trajectory Planning of Novel EOD Manipulator. *Appl. Sci.* **2021**, *11*, 9438. [[CrossRef](#)]
31. Li, K.; Huo, Y.; Liu, Y.; Shi, Y.; He, Z.; Cui, Y. Design of a lightweight robotic arm for kiwifruit pollination. *Comput. Electron. Agric.* **2022**, *198*, 107114. [[CrossRef](#)]
32. Zhu, H. Effect on Milking Performance Parameters and Cow Udder Health Between Rubber Liner and Silicone Liner. Master's Thesis, Nanjing Agricultural University, Nanjing, China, 2019. [[CrossRef](#)]
33. Gemini—Double Box Milking. Available online: [https://boumatic.com/us\\_en/products/gemini-the-boumatic-milking-robot-1-1-1/](https://boumatic.com/us_en/products/gemini-the-boumatic-milking-robot-1-1-1/) (accessed on 22 April 2023).
34. Kolbach, R.; Kerrisk, K.; Garcia, S. Short communication: The effect of premilking with a teat cup-like device, in a novel robotic rotary, on attachment accuracy and milk removal. *J. Dairy Sci.* **2013**, *96*, 360–365. [[CrossRef](#)]

**Disclaimer/Publisher's Note:** The statements, opinions and data contained in all publications are solely those of the individual author(s) and contributor(s) and not of MDPI and/or the editor(s). MDPI and/or the editor(s) disclaim responsibility for any injury to people or property resulting from any ideas, methods, instructions or products referred to in the content.